Journal of
Marine Science and Engineering

MDPI

Article

Dynamics of Water, Salt, and Nutrients Exchange at the Inlets of Three Coastal Lagoons

Maria Zoidou, Nikolaos Kokkos and Georgios Sylaios *

Laboratory of Ecological Engineering and Technology, Department of Environmental Engineering, Democritus University of Thrace, 67100 Xanthi, Greece; mzoidou@windowslive.com (M.Z.); nikolaoskokkos@gmail.com (N.K.)
* Correspondence: gsylaios@duth.gr; Tel.: +30-25410-79398; Fax: +30-25410-79393

Abstract: The intertidal patterns at the inlet of three coastal lagoons (Agiasma, Porto Lagos, and Xirolimni) in Northern Greece were investigated by combining in situ samplings and computational efforts. These lagoons are Mediterranean, microtidal coastal systems, connected with the adjacent open sea (Thracian Sea) through their inlet canals and are highly affected by the lagoon–sea exchange processes. Limited freshwater enters their basins, mostly due to precipitation and agricultural drainage. An intense monitoring program of water flow and quality at the mouth of the three lagoons was carried out, aiming to quantify the transport mechanisms of water, salt, and nutrients across the inlet canal under different tidal/meteorological conditions. Ebb currents were recorded higher than flood currents, and the temporal variability of the longitudinal velocity was characterized by asymmetries. Residual currents were important to the water exchange, with the Eulerian water, salt, and nutrient fluxes being an order of magnitude larger than the Stokes drift. Eulerian transport and tidal pumping are considered as important mechanisms for salt and nutrients exchange through the inlets. The return flow factor varied from 1 to 17.5% of the water exiting the lagoons in ebb, while the residence time ranged from 0.7 days to 4.2 days.

Keywords: water and salt balance; nutrients; residual currents; Stokes drift; residence time; Agiasma; Porto Lagos; Xirolimni

Citation: Zoidou, M.; Kokkos, N.; Sylaios, G. Dynamics of Water, Salt, and Nutrients Exchange at the Inlets of Three Coastal Lagoons. *J. Mar. Sci. Eng.* **2022**, *10*, 205. https://doi.org/10.3390/jmse10020205

Academic Editor: Ana Picado

Received: 13 January 2022
Accepted: 28 January 2022
Published: 2 February 2022

1. Introduction

Coastal lagoons are highly productive ecosystems important for the cycling of energy and nutrients. A series of key biogeochemical processes take place in the lagoon basins, such as net primary production, burial and remineralization of substances across the water-sediment interface, dissolving oxygen over-consumption towards benthic anoxia, and chemical exchange with the atmosphere [1,2]. Mediterranean lagoons provide key ecosystem services, such as human welfare and wellbeing, climate, water and natural hazard regulation, primary production, biotic diversity, habitat and food for bivalves, crustaceans, fish and birds, erosion prevention, and wild life refuge [1,3]. Moreover, a large fraction of the population living in the vicinity of these coastal systems depends largely on these ecosystems and receives their services [1]. However, lagoons are threatened mostly by humans, and the main causes of their degradation are pollution, water withdrawal, habitat destruction, overexploitation, invasive species, and climate change [4,5]. Information on coastal systems and their hydrodynamic processes is essential for their management and restoration [6].

Tidal inlets are usually narrow and shallow, and they transport seawater in and out of the main basin of the lagoon in accordance with the tide. During flood tidal phase, the sea level rises, and the pressure gradient results in the flow of water towards the lagoon; on the contrary, as the sea level lowers, the water flows out of the lagoon during the ebb tidal phase. The geometry of the inlet canal (length, width, depth) regulates the water flow

and the exchange characteristics of dissolved and particulate water contents between the lagoon basin and the open sea [7,8]. The water circulation within Mediterranean micro-tidal lagoons is mostly characterized by low tidal oscillations, on which residual (non-tidal) water circulations are superimposed [9]. Residual currents are influenced by internal tidal asymmetry due to bathymetric and topographic effects, winds, freshwater discharge, and freshwater-induced density gradients [10]. They have relatively low values (~0.1 m/s), but they play an important role in the shallow, coastal waters in transferring nutrients, pollutants, and sediments towards/from the adjacent sea [9,11,12]. Canals' geometry produces tidal asymmetry, leading to residual currents that cause net flow transport in the ebb or flood direction. In parallel, the transport of sediments, contaminants, and nutrients due to residual currents could impact the overall ecological state and the geomorphic processes of a coastal lagoon [12]. Based on the above, it is clear that the determination of water circulation patterns in lagoon canals and inlets is fundamental for the sustainable management of these systems and for the determination of the impact of human activities and climate change on them.

Lagoon exchange dynamics affect the water renewal processes of the lagoon basin and can be expressed by a series of metrics, namely residence time, age, flushing time, turnover time, and transit time. Takeoka [13] defined residence time of a Lagrangian water parcel at a given point in the lagoon as the time period spent in the lagoon basin before its exit towards the sea through the inlet, mostly during the ebb phase. In computationally intensive works, residence time can be estimated by hydrodynamic models, using tracers along with in situ water flow measurements [14,15]. In small, well-mixed embayments with limited freshwater influx, the classical tidal prism approach may be followed, considering that portion of the exited water parcel may re-enter the control domain during the consecutive flood [16–18]. Residence time is also an important indicator of the trophic state of a coastal system [8].

A series of sixteen coastal lagoons are situated at the deltaic zones of the Evros, Nestos, and Strymon Rivers and in the Vistonikos Gulf, northeastern Greece, forming four wetland complexes protected by the Ramsar Treaty [19]. These systems are fishery-exploited with permanent entrapment devices installed at their inlets to entrap fish during their inshore–offshore seasonal migration [20]. Three of these lagoons are studied in this work: Agiasma, Porto Lagos, and Xirolimni. They were selected on the basis of limited knowledge on exchange dynamics and their significant ecosystem services, such as the ecological/biodiversity values, fishery production, and recreation. The main objectives of the study are (a) to quantify the instantaneous and residual water, salt, chlorophyll, and nutrients fluxes across the lagoon inlet; (b) to compute nutrient loads from and to the open sea, thus identifying sources of pollution; (c) to apply a simple tidal prism model to estimate the lagoon's residence time under various tidal and meteorological conditions; and (d) to discuss the relative importance of physical processes (tidal, hydrologic, and meteorological) contributing to the overall exchange rate between the lagoon and the adjacent coastal water. Quantifying the exchange rates and fluxes at the inlets of these lagoons will aid fishery managers to increase fish production and improve ecosystem dynamics.

2. Materials and Methods

2.1. Study Area Description

Field campaigns were conducted in spring and summer 2016 and 2018, at the inlets of the three study lagoons (Agiasma, Port Lagos and Xirolimni), considering the meteorological and fortnight tidal variability (spring/neap cycles). During these surveys, water flow and physical parameters (water temperature, salinity, and water elevation) were measured, and water samples were collected during a series of consecutive tidal cycles. The geometric and hydrologic parameters for the three lagoons and their exchange inlets to the sea are summarized in Table 1. Agiasma is a shallow lagoon (mean depth 0.5 m), covering an area of 3.3 km^2, with its basin being about 7 km in length, 0.8 km in width, and a perimeter of 24.3 km. It is connected with the open sea through two narrow inlet channels, A and

B (Figure 1a). Previous studies [21] illustrate that water temperature varies from 6 °C in February to 30 °C in the summer, while the mean annual salinity is 30 psu.

Table 1. Geometric characteristics of Agiasma, Porto Lagos, and Xirolimni lagoons and their inlets.

	Agiasma	Porto Lagos	Xirolimni
Main Basin			
Geographic coordinates	24.612° E, 40.853° N: 24.625° E,40.913° N	25.133° E, 40.979° N: 25.168° E, 41.011° N	25.138° E, 40.951° N: 25.158° E, 40.968° N
Mean depth (m)	0.50	0.52	0.52
Effective mean depth (m)	0.59	0.68	1.13
Perimeter (km)	24.3	20.7	6.4
Area (km^2)	3.33	3.75	1.76
Volume (km^3)	1.66×10^{-3}	1.37×10^{-3}	9.00×10^{-4}
Minimum depth (m)	0.10	0.10	0.10
Maximum depth (m)	4.45	4.33	4.00
Inlet A			
Length (m)	182.0	1100.0	318.5
Mean width (m)	19.5	13.2	16.1
Mean depth (m)	0.50	0.78	0.26
Inlet B			
Length (m)	418.6	37.0	-
Mean width (m)	25.7	8.70	-
Mean depth (m)	0.54	0.26	-

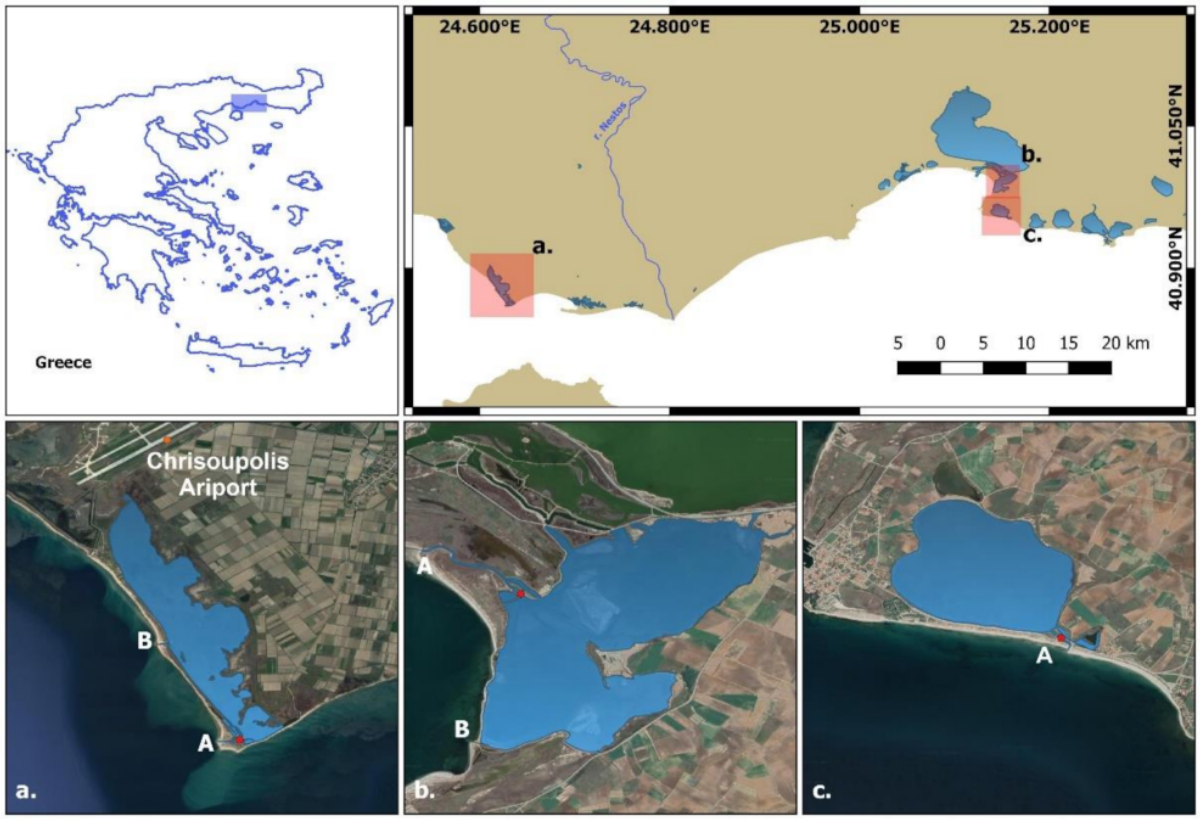

Figure 1. Map of the three lagoons under study, showing the location of the current meter and the CTD probe (red dots): (**a**) Agiasma, (**b**) Porto Lagos, and (**c**) Xirolimni.

The eastern part of Porto Lagos lagoon is shallow with a mean depth of 0.5 m, and it covers an area of 3.75 km^2. The lagoon receives brackish water from Vistonis lagoon and communicates with the Thracian Sea with two inlets, A and B (Figure 1b). Seasonal variability in water temperature shows fluctuation from 6 °C in December to 30 °C in August. Salinity ranges between 0.5 in spring and 36 psu in summer months.

Xirolimni lagoon has an average depth of 0.6 m, covering an area of 1.8 km^2. It connects to the sea with a narrow, 320-m long inlet along a NW–SE direction (inlet A, Figure 1c). The lagoon water temperature ranges from 4 °C in February to 30 °C in summer. Salinity reaches its maximum value during July (S = 46 psu) and reduces to 12 psu in November.

In Agiasma and Xirolimni, the direct freshwater inputs are minimal except from precipitation and agricultural runoff, especially during flash flood events. All three lagoons are surrounded by cultivated fields (mostly cotton, maize, alfalfa). Lagoons are forced by similar tidal influence (spring tidal range 0.3 m and neap tidal range 0.1 m) at their entrance canals, and all belong to the same Koppen climatic zone (Csb, warm summer Mediterranean climate). Mean annual precipitation is around 320 mm, ranging between 420–430 mm and air temperature between –5 °C and 38 °C, with mean air temperature around 15 °C. In the North Aegean Sea, the dominant winds blow from the north and northeast directions, while south-southwestern winds prevail in spring and summer.

2.2. Equipment and Data Collection

The data set consists of three complete tidal cycles (29 September 2016–01 October 2016) for Agiasma lagoon, three tidal cycles within the period of June–July 2018 for Porto Lagos, and fifteen tidal cycles (July 2016 and April–May 2018) for Xirolimni, under various tidal and meteorologic conditions.

Water flow was measured using a Valeport Model 106 self-recording current meter, operating at 5-min intervals, deployed at the inlet of each lagoon as shown in Figure 1. Water temperature, salinity, and tidal elevation were measured using a Midas Valeport CTD probe. Meteorological parameters were obtained (wind speed, wind direction, precipitation) from the nearby airport (Chrisoupolis Airport).

Water samples were collected at each sampling point every three hours, filtered immediately after their collection, frozen, and stored for nutrient determination. The methods used for nitrates, nitrites, total phosphorus (TP), o-phosphates, and chlorophyll-a (chl-a) determination are shown in Table 2. For the consecutive analysis of nutrient fluxes, the sum of nitrites, nitrates, and ammonium concentration was considered as the dissolved inorganic nitrogen (DIN) concentration.

Table 2. Methods used for the determinations of the nutrients, chlorophyll-a, and total suspended solids.

Parameters	Methods
Nitrates	Cadmium reduction method (4500-NO3- E) [22]
Nitrites	Colorimetric method (4500-NO2- B) [22]
Total phosphorus (TP)	Ascorbic acid method (4500-P B and E) [22]
O-phosphates	Ascorbic acid method (4500-P E) [22]
Chlorophyll-a (Chl-a)	Spectrophotometric determination (10200 H) [22]

2.3. Estimation of the Water, Salt, and Nutrient Fluxes

The water flow was measured by defining a longitudinal axis oriented along the entrance inlet, with the positive part towards the lagoon and a lateral axis positive to the right. The instantaneous rate of water transport per unit of width through a water column of depth H, Q (m^3/(ms)), was estimated following Sylaios, et al. [9].

$$Q = H\overline{U} = H(\overline{u}, \overline{v}) \quad (1)$$

where u, v (m/s) are the components of the longitudinal U velocity in the x, y directions, respectively. The overbar indicates an average over depth.

The depth-integrated residual transport of water at the mouth of a lagoon is the result of flows due to the depth-averaged Eulerian residual current (the non-tidal drift) and the mass transport Stokes drift (the tidal pumping of water), linked to the non-zero correlation between tidal fluctuations in water depth and velocity [23]. The residual rate of water transport is given by:

$$\langle Q \rangle = \langle H \rangle (V_1 + V_2) \tag{2}$$

where, $\langle n \rangle$ is the tidal average of a variable; here, $\langle H \rangle$ is the tidally-averaged depth of the water column (m); V_1 is the depth-averaged Eulerian residual transport (m/s), expressed by Dyer and Lasta King [24] as:

$$V_1 = \langle \overline{U} \rangle \tag{3}$$

and V_2 (m/s) is the mass transport Stokes drift transport (residual rate of transport of water from tidal pumping), expressed as [25,26]:

$$V_2 = \left\langle \widetilde{H}\widetilde{U} \right\rangle / \langle H \rangle \tag{4}$$

where $\widetilde{H}$ and $\widetilde{U}$ are the depth-averaged instantaneous deviation of depth and velocity from the tidal mean, respectively.

Likewise, the instantaneous transport rate of salt, Q_S (g/(ms)), per unit of inlet width through a water column of depth H is given as:

$$Q_S = H\overline{US} \tag{5}$$

The residual transport rate of salt is calculated by:

$$\langle Q_S \rangle = \langle H \rangle (V_{S,1} + V_{S,2} + V_{S,3}) \tag{6}$$

where $V_{s,1}$ (g/(m^{2}s)) is the depth-averaged residual flux of salt due to the residual transport of water, expressed as:

$$V_{S,1} = \langle Q \rangle \langle \overline{S} \rangle / \langle H \rangle \tag{7}$$

$V_{s,2}$ (g/(m^{2}s)) is the depth-averaged residual flux due to tidal pumping, expressed as:

$$V_{S,2} = \left\langle \widetilde{Q}\widetilde{S} \right\rangle / \langle H \rangle \tag{8}$$

$V_{s,3}$ (g/(m^{2}s)) is the depth-averaged residual flux of salt due to the vertical shear between the tidal and residual currents, which is expressed as:

$$V_{S,3} = \left\langle H\overline{U'S'} \right\rangle / \langle H \rangle \tag{9}$$

where U' and S' represent the deviations of velocity and salinity from the depth averaged value, respectively. At the three lagoons under study, the water column is considered as well mixed, and thus, term $V_{s,3}$ is negligible ($S' \sim 0$).

Similarly, the instantaneous and residual transport rates of any water constituent (e.g., nutrients, chlorophyll-a) were calculated using the Equations (5) to (9) by replacing salinity with the appropriate water constituent concentrations [27].

The volume of flood and ebb water was computed for each tidal cycle by:

$$Flood\ Volume(y) = \int_{t=0}^{t=\tau} Q dt \tag{10}$$

and

$$Ebb\ Volume(y) = \int_{t=\tau}^{t=T} Q dt \tag{11}$$

in which *FloodVolume(y)* or *EbbVolume(y)* (m^3/m) represent the respective tidal prisms during flood or ebb period per meter of width; T is the tidal period (45,000 s); and $t = 0$, $t = \tau$, and $t = T$ represent the slack tidal times.

The lagoon tidal prism *PrismVolume* (m^3/m) is equal to $(Flood\ Volume + Ebb\ Volume)/2$, and by multiplying the *PrismVolume* with the width of each entrance channel, the lagoon tidal prism V_{Prism} (m^3) is produced.

2.4. Residence Time Estimation

The residence time of the three lagoons was estimated using the tidal prism model described by Luketina [17]. Agiasma, Porto Lagos, and Xirolimni lagoons are considered as well-mixed systems receiving limited amounts of fresh water.

The average fraction, f, of fresh water by volume is expressed by:

$$\left(V_{Lagoon} + V_{Prism}\right)S_{HW} = (1 - f)\left(V_{Lagoon} + V_{Prism}\right)S_{OC} \Rightarrow f = 1 - \frac{S_{HW}}{S_{OC}} \tag{12}$$

where V_{Lagoon}, is the volume of the lagoon (m^3); V_{Prism} is the lagoon tidal prism volume (m^3); S_{HW} is the salinity in the lagoon at high tide; and S_{OC} is the mean salinity of the open sea adjacent to the lagoon.

The freshwater volume V_R (m^3) entering the lagoon during a tidal cycle is given by:

$$V_R = fV_{Prism} \tag{13}$$

and the fresh water inflow Q_R (m^3/s) to the tidal flow is typically expressed by:

$$Q_R = V_R/T \tag{14}$$

where T is the tidal period (s).

For a lagoon in steady state, the salinity at high tide (S_{HW}) is estimated by Luketina [17]:

$$S_{HW} = \frac{\sin\vartheta - \frac{Q_R T}{\pi V_{Prism}}(\pi - \vartheta)}{\sin\vartheta + \frac{Q_R T}{\pi V_{Prism}}\left(\frac{\vartheta + b(\pi - \vartheta)}{1 - b}\right)} S_{OC} \tag{15}$$

where θ describes the flood and ebb flow lags because of the presence of river flow:

$$\theta = \cos^{-1}\left(\frac{Q_R T}{\pi V_{Prism}}\right) \tag{16}$$

and b is the return flow factor, the fraction of returning water that left the lagoon during ebb and re-enters during flood [16]. The return flow factor, b, can range from 0 to 1. A return flow factor close to 0 means the lagoon is well flushed, typically by alongshore currents; hence, only a small fraction of water returns to the lagoon during flood.

When the normalized river flow $\frac{Q_R T}{\pi V_{Prism}}$ is much less than 1, then θ is around 1, so the salinity at high tide is given by:

$$S_{HW} = \frac{V_{Prism} - \frac{Q_R T}{2}}{V_{Prism} + \frac{Q_R T}{2}\left(\frac{1+b}{1-b}\right)} S_{OC} \tag{17}$$

The equation above is to produce the parameter of return flow factor, b, for the sampled tidal cycles based on observed values of S_{HW} and S_{OC}.

The lagoon's residence time based on Luketina's corrected tidal prism method can therefore be calculated as

$$t_{RES} = \frac{V_{Lagoon} + V_{Prism}}{(1 - b)\frac{V_{Prism}}{T} + (1 + b)\frac{Q_R}{2}} \tag{18}$$

2.5. Exchange Dynamics

The effects of the wind and tides on the salt dynamics through the mouth of shallow Mediterranean lagoons were estimated according to Hearn and Robson [28]. Barotropic tidal exchange is induced by the difference in the external water level due to astronomical tides, the difference in barometric pressure, and the wind shear stress. The barotropic tidal exchange rate R_{Tide} is calculated by:

$$R_{Tide} = \frac{\mu}{t_{Tide}} \frac{V_{Prism}}{V_{Lagoon}} \quad (19)$$

where μ is the retention coefficient ($\mu = 1 - \frac{V_{Channel}}{V_{Prism}}$); V_{Prism}, the tidal prism; $V_{Channel}$, the volume of the entrance canal; V_{Lagoon}, the volume of the lagoon basin; and t_{Tide}, the dominant tidal period.

The baroclinic tidal exchange is equal to:

$$R_{Baroclinic} = \frac{A_C \sqrt{\frac{\Delta\rho}{\rho} g h_{Channel}}}{4V_{Lagoon}} \quad (20)$$

where A_c is the cross-section area of the channel; $\Delta\rho$, the density difference between the two ends of the entrance canal; ρ, the mean water density; $h_{Channel}$, the average depth of the channel; and g, the acceleration due to gravity.

The wind-induced exchange is given by:

$$R_{Wind} = \frac{\mu}{t_{Wind}} \frac{V_{Wind}}{V_{Lagoon}} \quad (21)$$

where t_{Wind} is the period of wind forcing and V_{wind} the volume exchange produced by wind, calculated by:

$$V_{Wind} = \frac{V_{Lagoon} \Delta\eta}{2H} \quad (22)$$

where H is the mean lagoon depth and $\Delta\eta$ the elevation difference between the two ends of the entrance canal, given by:

$$\Delta\eta = \frac{\beta C w \rho_{air} L}{\rho g H} UW \quad (23)$$

where β is the fraction of wind stress that is balanced by pressure gradient (~0.8); C_W, the wind drag coefficient (=0.002); ρ_{air}, the air density (=1.2 kg/m^3); L, the length of the lagoon basin; U, the longitudinal component of wind vector; and W, the wind speed.

3. Results

3.1. Water Flow and Water Properties Variability

3.1.1. Agiasma Lagoon

The hydrographic parameters for Agiasma lagoon are summarized in Table 3. All three tidal cycles under study refer to spring tidal conditions, where the tidal range varied from 0.06 m to 0.11 m, with the semi-diurnal constituent, M_2, being the dominant. The tidal cycle duration ranged from 10.6 to 13.7 h, with the ebb duration being higher than the flood. The north wind seems to increase the ebb duration (29 September 2016, 30 September 2016) compared to the flood. Zero precipitation was experienced during the sampling period. Ebb currents were stronger than the flood currents. Average and maximum ebb flow speeds ranged from 0.13–0.15 m/s and 0.18–0.20 m/s, respectively, while the flood ones were significantly lower. Figure 2 illustrates the temporal variability of the longitudinal velocity, tidal elevation, and salinity at the mouth of Agiasma lagoon during the three spring tidal cycles. The longitudinal velocity follows the semi-diurnal motion, and the flood and ebb phases are well defined.

Table 3. Tidal parameters and meteorological conditions during the three tidal cycles sampled at the Agiasma lagoon inlet at (1) 29 September 2016, (2) 30 September 2016, and (3) 30 September 2016.

Tidal Parameter	1	2	3
Mean wind speed (m/s)	1.00	1.12	1.26
Wind direction	N	S-SW	N-NE
Precipitation (mm)	0.00	0.00	0.00
Average depth (m)	0.63	0.62	0.59
Tidal phase	S	S	S
Tidal range (m)	0.11	0.06	0.11
Tidal duration (min)	790	635	820
Ebb duration (min)	450	350	480
Time to max ebb (min)	270	110	295
Max ebb (m/s)	0.20	0.18	0.20
Mean ebb (m/s)	0.14	0.15	0.13
Flood duration (min)	340	285	340
Time to max flood (min)	80	50	135
Max flood (m/s)	0.05	0.04	0.03
Mean flood (m/s)	0.02	0.01	0.01
Tidal mean (m/s)	−0.067	−0.079	−0.073

S, spring tide; N, neap tide.

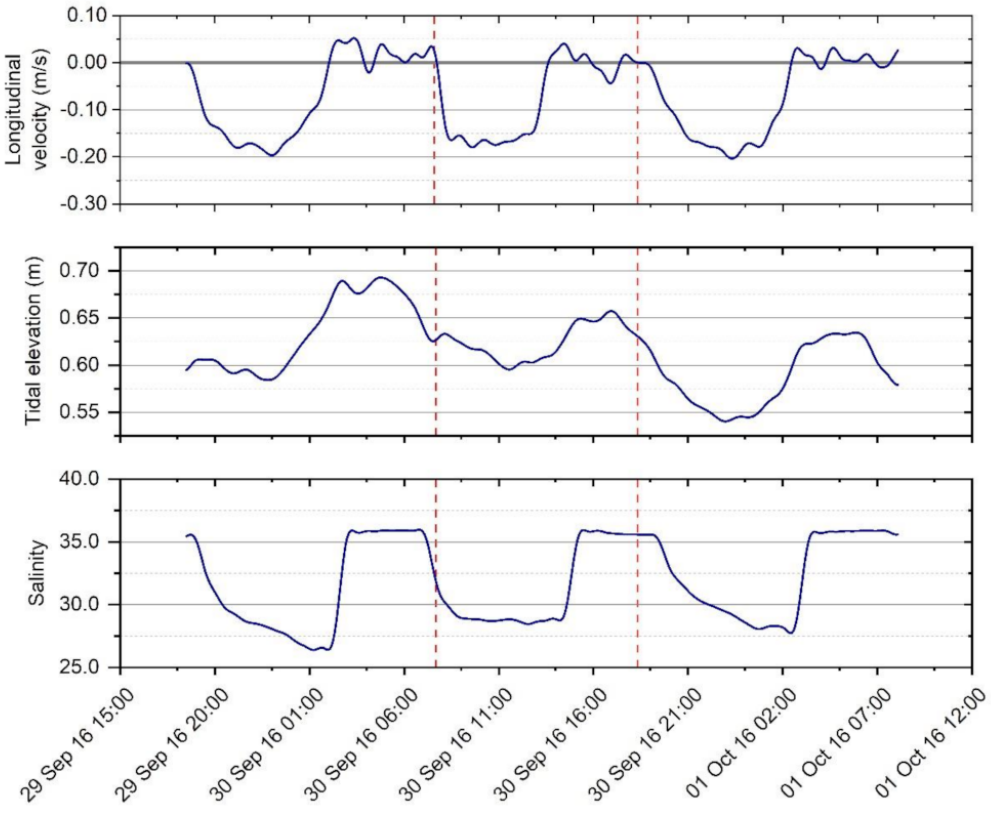

Figure 2. Temporal variability of longitudinal velocity, tidal elevation, and salinity at the inlet of Agiasma lagoon during the three cycles under study. The red dashed lines indicate the duration of each tidal cycle.

The salinity pattern is influenced by the permanent exchanges with the adjacent sea. The highest values occur during the flood (35.9) and the lowest values during ebb (26.2–28.4). The lowest salinity values are observed during low tide (at the end of the ebb phase), as the water flows out of the lagoon to the sea.

In Agiasma lagoon, only two cycles were sampled for nutrients (29 September 2016 and 30 September 2016). During the first cycle (29 September 2016), concentrations in all

water quality parameters were found higher in ebb, with the exception of total phosphorus exhibiting the reverse behavior. In the second cycle (30 September 2016), DIN concentration values were higher during ebb, and total phosphorus, phosphates, chlorophyll-a were lower (Table 4). Chlorophyll-a concentration was moderate to high. DIN concentration ranged from 60 μg/L to 120 μg/L for the sampled cycles (ammonium is almost 50% of the total dissolved inorganic nitrogen, nitrates 49%, and nitrites 1%). Phosphates were low, with the maximum value reaching 22 μg/L on 29 September 2016.

Table 4. Concentration of nutrients and chlorophyll-a during ebb and flood for the sampled tidal cycles.

Tidal Cycle		Tidal Phase	Parameter			
			DIN (μg/L)	Total Phosphorus (μg/L)	Phosphates (μg/L)	Chlorophyll-a (μg/L)
Agiasma						
29 September 2016	S	Ebb	107.22	66.40	8.10	2.39
		Flood	95.94	78.26	3.54	2.00
30 September 2016	S	Ebb	83.27	39.49	4.81	2.49
		Flood	63.81	42.67	5.80	3.07
Porto Lagos						
26 June 2018	S	Ebb	259.97	61.76	0.00	4.17
		Flood	202.50	41.57	0.00	1.36
06 July 2018	N	Ebb	162.29	72.57	0.00	7.58
		Flood	205.86	95.65	0.00	20.40
10 July 2018	N	Ebb	104.91	96.37	0.00	36.28
		Flood	128.55	178.56	1.35	28.57
Xirolimni						
19 July 2016	S	Ebb	107.41	82.92	53.26	0.88
		Flood	92.67	49.66	0.99	0.65
26 July 2016	N	Ebb	190.75	42.03	28.04	1.39
		Flood	123.52	21.06	14.46	2.45
30 April 2018	S	Ebb	82.73	21.38	0.00	0.05
		Flood	79.40	13.58	2.94	0.15
01 May 2018	S	Ebb	139.55	55.27	0.00	0.14
		Flood	281.79	64.64	9.74	0.66
01 May 2018	S	Ebb	247.56	190.10	5.13	0.24
		Flood	292.12	101.41	27.04	0.14

Nutrient and chlorophyll-a import and export loads were estimated by multiplying the flood and ebb mean concentrations with the respective flood and ebb tidal volumes. Results are shown in Figure 3, from which it is evident that the mean ebb exports are significantly higher than the mean flood loads.

3.1.2. Porto Lagos lagoon

Table 5 summarizes the observed tidal characteristics and meteorological conditions for each of the three tidal cycles under study in Porto Lagos lagoon. The first cycle (26 June 2018) represents a typical spring tidal condition, while the other two represent tidal neaps. The tidal range varied from 0.07 m to 0.11 m, and the cycle duration ranged from 10.3 h to 14.2 h. Ebb duration (8 h) was higher than flood duration (6.2 h) during the cycle under spring conditions and lower for the cycles under neap conditions (ebb duration: 3.6 to 4.9 h, flood duration: 6.8 to 6.9 h). Additionally, max ebb currents were stronger than the max flood currents, while the mean values were almost equal. Max flood flow speeds varied from 0.06 to 0.08 m/s during neap tides and 0.14 m/s during spring tide, and max ebb flow speeds varied from 0.08 to 0.11 m/s during neap tides and 0.27 m/s during spring tide.

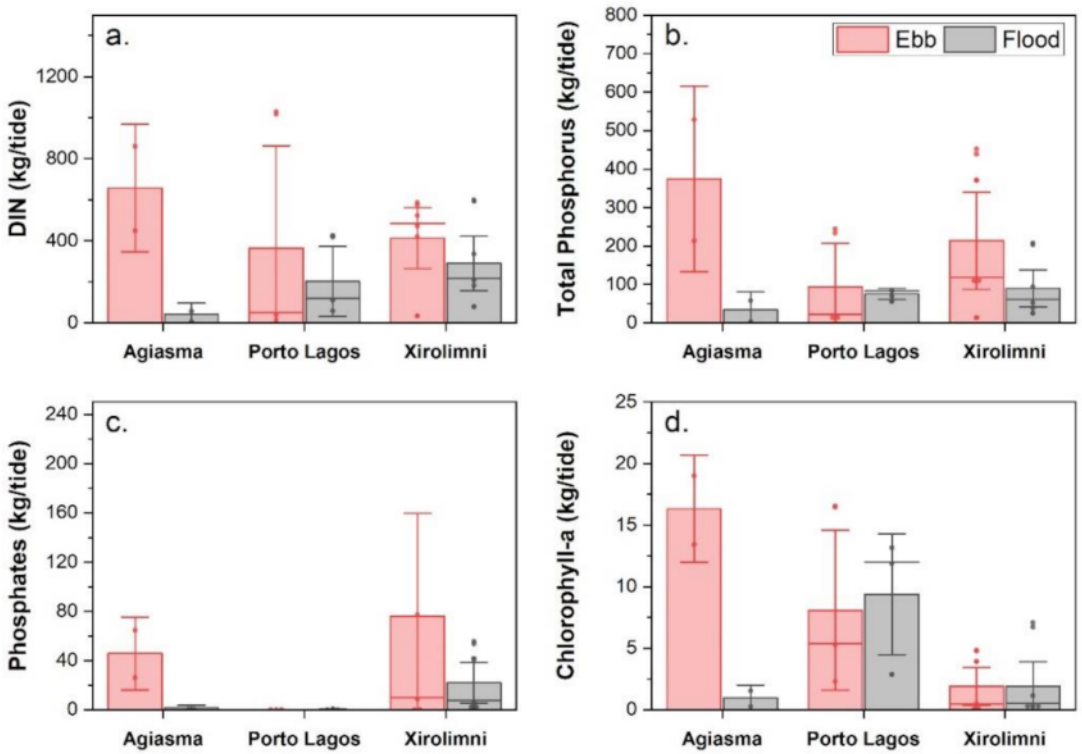

Figure 3. Ebb (red bars) and flood (grey bars) for nutrient and chlorophyll-a loads during the sampled tidal cycles: (**a**) dissolved inorganic nitrogen, (**b**) total phosphorus, (**c**) phosphates and (**d**) chlorophyll-a.

Table 5. Tidal parameters and meteorological conditions of the three tidal cycles sampled at the Porto Lagos lagoon inlet at (1) 26 June 2018, (2) 6 July 2018, and (3) 10 July 2018.

Tidal parameter	1	2	3
Mean wind speed (m/s)	5.40	1.84	1.80
Wind direction	NE	N	N-NE
Precipitation (mm)	0.01	0.00	0.00
Average depth (m)	0.49	0.20	0.29
Tidal phase	S	N	N
Tidal range (m)	0.11	0.11	0.07
Tidal duration (min)T	850	710	620
Ebb duration (min) t_{Ebb}	480	295	215
Time to max ebb (min) $t_{max.\ Ebb}$	175	135	145
Max ebb (m/s) $u_{max.Ebb}$	0.27	0.11	0.08
Mean ebb (m/s)	0.10	0.06	0.04
Flood duration (min) t_{Flood}	370	415	405
Time to max flood (min) $t_{max.\ Flood}$	185	255	245
Max flood (m/s)$u_{max.\ Flood}$	0.14	0.08	0.06
Mean flood (m/s)	0.10	0.05	0.03
Tidal mean (m/s)	–0.016	0.003	0.007

S, spring tide; N, neap tide.

Figure 4 presents the temporal variability of the longitudinal velocity, tidal elevation, and salinity at the mouth of Porto Lagos lagoon during a spring tide (26 June 2018) and a neap tide cycle (10 July 2018). The longitudinal velocity follows the semi-diurnal pattern, and the flood and ebb phases are well defined. The highest salinity values occur during flood (33.7–38.5) and the lowest during ebb (31.3). During the spring tide cycle, the highest intra-tidal salinity difference is observed (~7).

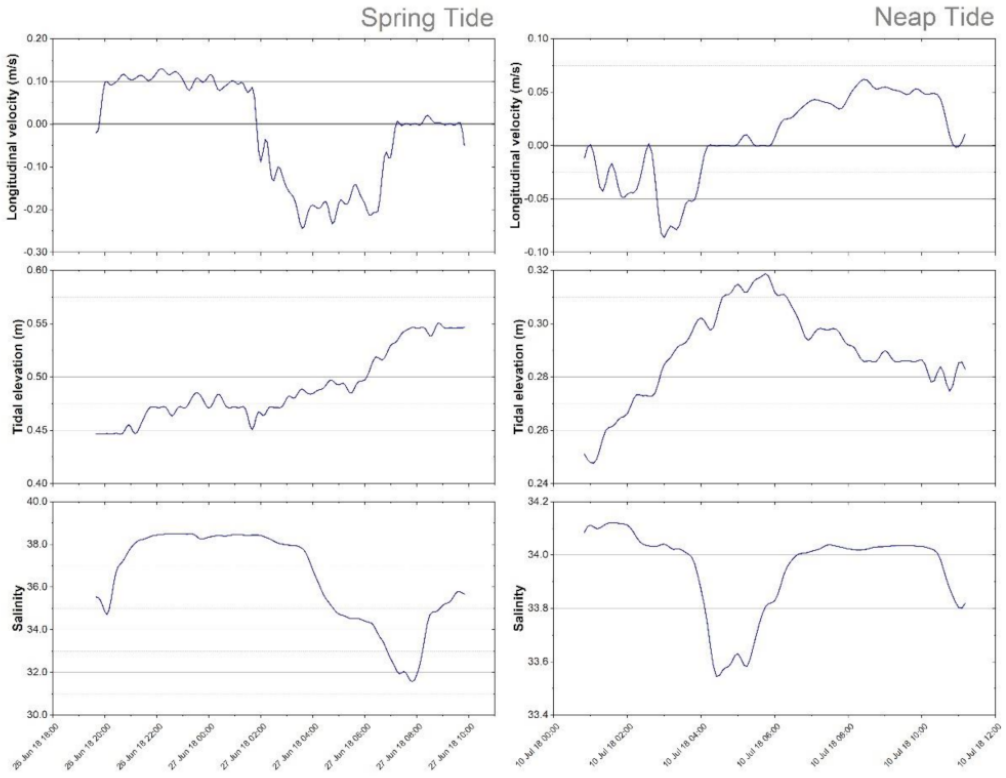

Figure 4. Temporal variability of longitudinal velocity, tidal elevation, and salinity at the inlet of Porto Lagos lagoon during 26 June 2018, spring tidal cycle, and 10 Jule 2018, neap tidal cycle.

Mean values of water-quality parameters for the sampled tidal cycles are presented in Table 4, and the loadings for those parameters are shown in Figure 3. During the first cycle (spring tide), the nutrient concentrations are higher during ebb tide. For the second (06 July 2018) and third (10 July 2018) cycles (neap tides), the flood nutrient loads were significantly higher compared to the ebb loads. Chlorophyll-a concentrations were extremely high, typical for spring and summer conditions, suggesting that the waters were probably under phytoplankton blooms. DIN concentration reached 120 μg/L, and total phosphorus reached 180 μg/L (ammonium is almost 78%, nitrates 21%, and nitrites 2%). Phosphates were undetectable. Mean nutrient ebb exports are higher than the flood loads in contrast to chlorophyll-a fluxes, which are affected by the chlorophyll-rich Vistonikos Gulf.

3.1.3. Xirolimni Lagoon

Table 6 summarizes the measured parameters for each tidal period in Xirolimni lagoon. In general, the tidal range in Xirolimni lagoon varied from 0.05 m to 0.1 m under spring and neap conditions, with tidal elevation following the semi-diurnal behavior. Flood duration varied from 3.3 to 7.5 h. The maximum ebb currents were stronger than the maximum flood currents. The average ebb currents were also stronger except for four tidal cycles (27 July 2016, 28 April 2018, 29/04/2018, and 01 May 2018). Furthermore, a typical inward speed is about 0.07 m/s during spring tide and 0.08 m/s during neap tide, and an ebb flow speed is about 0.13 m/s during spring tide and 0.11 m/s during neap tide.

Following a representative spring tidal cycle (27 July 2018), ebb has a duration of 6.8 h, a maximum ebb speed of 0.22 m/s, and an average ebb speed of 0.14 m/s. Flood lasts for 6.1 h, the maximum flood speed is 0.10 m/s, and the average flood speed is 0.07 m/s.

Under neap tide conditions (26 July 2016), the ebb duration is 5.4 h, maximum ebb speed is 0.23 m/s, and average ebb speed is 0.16 m/s. Flood lasts for 7.3 h, has a maximum flood speed of 0.13 m/s, and an average flood speed of 0.09 m/s.

Table 6. Tidal parameters and meteorological conditions of each tidal cycle sampled at the Xirolimni lagoon inlet at (1) 19 July 2016, (2) 20 July 2016, (3) 20 July 2016, (4) 26 July 2016, (5) 26 July 2016, (6) 27 July 2016, (7) 27 April 2018, (8) 28 April 2018, (9) 28 April 2018, (10) 29 April 2018, (11) 29 April 2018, (12) 30 April 2018, (13) 30 April 2018, (14) 01 May 2018, and (15) 01 May 2018.

Tidal Parameter	1	2	3	4	5	6	7	8	9	10	11	12	13	14	15
Mean wind speed (m/s)	3.91	4.07	3.45	4.38	5.68	3.18	4.03	4.70	5.44	4.73	3.33	2.43	1.46	2.70	2.29
Wind direction	N-NE	NE	NE	NE	NE	N-NE	N-NE	NE-E	NE	NE-E	NE	S-SW	E	SW	NE-E
Precipitation (mm)	0.00	0.00	0.00	0.00	0.00	0.00	0.00	0.00	0.00	0.00	0.00	0.00	0.00	0.00	0.00
Average depth (m)	0.53	0.55	0.56	0.52	0.58	0.56	0.41	0.42	0.41	0.41	0.42	0.41	0.42	0.42	0.43
Tidal phase	S	S	S	N	N	N	S	S	S	S	S	S	S	S	S
Tidal range (m)	0.10	0.09	0.09	0.05	0.10	0.05	0.09	0.10	0.05	0.09	0.05	0.05	0.07	0.06	0.07
Tidal duration $(\mathrm{min}) T$	835	705	770	765	710	730	715	775	745	780	755	670	730	700	755
Ebb duration $(\mathrm{min}) t_{Ebb}$	435	485	405	325	290	315	265	355	345	505	480	475	410	415	345
Time to max ebb $(\mathrm{min}) t_{max.\ Ebb}$	125	200	280	85	110	30	115	85	165	105	230	240	250	55	70
Max ebb $(\mathrm{m/s}) u_{max.Ebb}$	0.25	0.31	0.22	0.23	0.20	0.20	0.22	0.22	0.21	0.24	0.43	0.24	0.33	0.17	0.22
Mean ebb (m/s)	0.17	0.21	0.14	0.16	0.12	0.05	0.15	0.06	0.11	0.06	0.15	0.09	0.23	0.01	0.12
Flood duration $(\mathrm{min}) t_{Flood}$	400	220	365	440	420	415	450	420	400	275	275	195	320	285	410
Time to max flood $(\mathrm{min})\ t_{max.\ Flood}$	100	95	170	130	155	105	205	145	165	125	115	90	90	125	200
Max flood $(\mathrm{m/s}) u_{max.\ Flood}$	0.11	0.07	0.10	0.13	0.13	0.13	0.14	0.14	0.14	0.11	0.10	0.10	0.12	0.10	0.14
Mean flood (m/s)	0.08	0.03	0.07	0.09	0.07	0.09	0.09	0.10	0.08	0.07	0.07	0.05	0.08	0.07	0.09
Tidal mean	−0.053	−0.132	−0.040	−0.014	−0.007	0.031	0.000	0.026	−0.012	−0.016	−0.073	−0.046	−0.094	−0.022	−0.002

S, spring tide; N, neap tide.

Figure 5 presents the temporal variability of the longitudinal velocity, tidal elevation, and salinity at the mouth of Xirolimni lagoon during nine spring and three neap tide cycles. Flood and ebb phases seem well defined. Salinity follows a semi-diurnal pattern, showing the highest values during flood phase although its values seem to drop at the end of the ninth spring tide cycle (Figure 5). The gradual drop in salinity appeared associated with the entry and expansion of the lower-salinity Black Sea water, covering the surface layer of the Thracian Sea continental shelf.

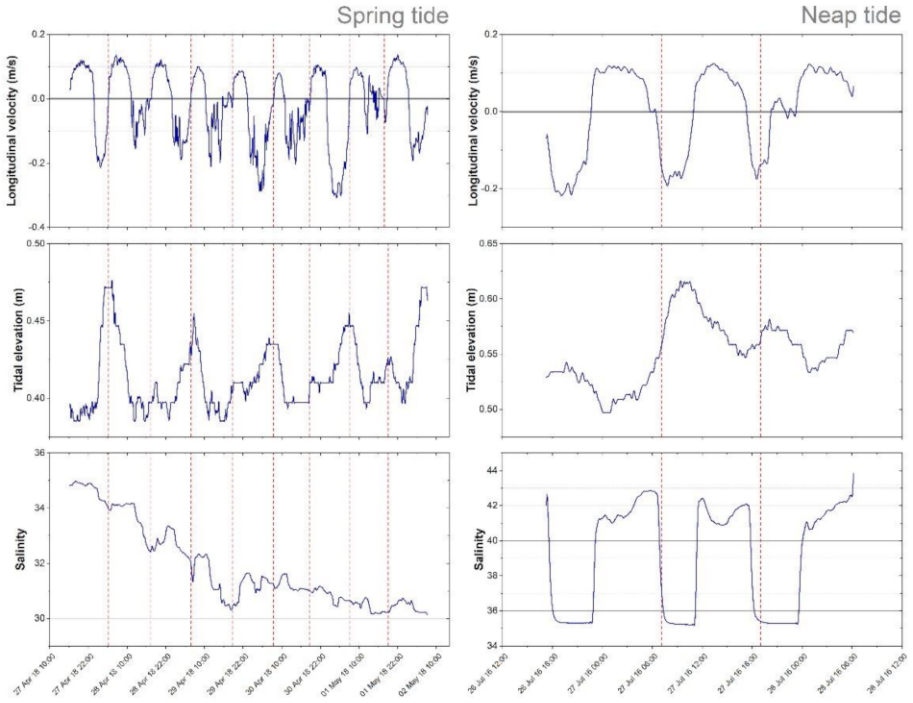

Figure 5. Temporal variability of longitudinal velocity, tidal elevation, and salinity at the inlet of Xirolimni lagoon during nine spring tidal cycles (27 April 2018—01 May 2018) and three neap tidal cycles (26 July 2016–27 July 2016). The red dashed lines indicate the duration of each tidal cycle.

Mean values of water-quality parameters for the sampled tidal cycles are presented in Table 4 and the respective fluxes for those parameters in Figure 3. For Xirolimni lagoon, nutrient concentrations are only available for five tidal cycles (19 July 2016, 26 July 2016, 30 April 2018, 01 May 2018, and 01 May 2018). During cycles 1 and 2 (19 July 2016 and 26 July 2016) (Table 4), all parameters were found higher during the ebb phase except for chlorophyll-a. During the 01 May 2018 cycle, the flood nutrient concentration was higher than the corresponding ebb. Chlorophyll-a concentration was low, except for the spring tidal cycle on 26 July 2016, when the chlorophyll-a concentration exceeded 1 μg/L. Higher values of DIN and total phosphorus were detected during spring 2018 (DIN mean value: 194 μg/L, TP mean value: 76 μg/L, ammonium is almost 78%, nitrates 21%, and nitrites 2%). As in Xirolimni, chlorophyll-a loads (Figure 5d) are affected by the highly productive waters of Vistonikos Gulf. On the other hand, mean nutrient ebb exports are found higher than the flood loads.

3.2. Residual currents

The residual fluxes and transport rates of water, salt, and nutrients at the inlet of the lagoons under study are illustrated in Tables 7 and 8. They were calculated from Equations (2)–(4) and (6)–(9). The Eulerian residual current, V_1, has an absolute mean value of 0.073 m/s for Agiasma, 0.009 m/s for Porto Lagos, and 0.038 m/s for Xirolimni. For Agiasma, the V_1 current was negative for the three sampled cycles; hence, the water flows out of the lagoon, while the other two lagoons had variable directions. It appears that the

negative Eulerian currents have higher absolute values, producing an absolute mean of 0.016 m/s for Porto Lagos and 0.044 m/s for Xirolimni, almost double the corresponding positive values (0.008 m/s for Porto Lagos and 0.023 m/s for Xirolimni).

Table 7. Residual fluxes and total transport rates (per unit of width) of water and salt during the sampled tidal cycles at the mouths of the three lagoons under study.

Date	Tidal Phase	Water Residual Fluxes			Salt Residual Fluxes		
		V_1 (m/s)	V_2 (m/s)	<Q> (m^3(s m))	$V_{s,1}$ (g/(m^2 s))	$V_{s,2}$ (g/(m^2 s))	<Qs> (g/(m^2 s))
Agiasma							
29 September 2016	S	−0.067	0.005	−0.040	−1.976	0.234	−1.105
30 September 2016	S	−0.079	0.002	−0.048	−2.410	0.167	−1.402
30 September 2016	S	−0.073	0.004	−0.040	−2.212	0.195	−1.187
mean		0.073	0.004	0.043	2.199	0.199	1.231
Porto Lagos							
26 June 2018	S	−0.016	−0.002	−0.009	−0.678	0.099	−0.284
06 July 2018	N	0.003	0.005	0.002	0.273	0.022	0.059
10 July 2018	N	0.008	0.0005	0.002	0.274	0.0001	0.079
mean		0.009	0.003	0.004	0.408	0.040	0.141
Xirolimni							
19 July 2016	S	−0.053	0.001	−0.028	−1.921	0.314	−0.855
20 July 2016	S	−0.132	−0.007	−0.076	−4.937	0.081	−2.658
20 July 2016	S	−0.040	0.0001	−0.022	−1.523	0.310	−0.677
26 July 2016	N	−0.014	−0.003	−0.009	−0.664	0.359	−0.159
27 July 2016	N	−0.007	−0.002	−0.005	−0.331	0.281	−0.029
27 July 2016	N	0.031	−0.001	0.017	1.148	0.202	0.753
27 April 2018	S	0.0003	−0.006	−0.002	−0.212	0.030	−0.074
28 April 2018	S	0.026	0.005	0.013	1.042	0.024	0.446
28 April 2018	S	−0.012	−0.002	−0.005	−0.435	0.013	−0.171
29 April 2018	S	−0.016	0.003	−0.005	−0.424	0.023	−0.163
29 April 2018	S	−0.072	−0.001	−0.031	−2.298	−0.012	−0.962
30 April 2018	S	−0.046	0.002	−0.018	−1.369	0.004	−0.554
30 April 2018	S	−0.094	−0.003	−0.041	−2.991	0.030	−1.245
01 May 2018	S	0.022	0.001	0.010	0.705	0.003	0.294
01 May 2018	S	−0.002	−0.004	−0.003	−0.183	0.011	−0.073
mean		0.038	0.003	0.019	1.346	0.113	0.608

Positive values represent fluxes towards the lagoon and negative values away from the lagoon.

Agiasma lagoon showed the highest Eulerian residual current during the 30/09/2016 spring tidal cycle (0.073 m/s). In Porto Lagos lagoon, the highest Eulerian water flux was obtained on 26 June 2018 under a spring tide cycle (−0.016 m/s) and the lowest on 06 July 2018 under a neap tide cycle (0.003 m/s). In Xirolimni lagoon, the highest Eulerian water flux was obtained on 20 July 2016 under a spring tide cycle (−0.132 m/s); this was the highest value observed during this study, while the lowest on 27 April 2018 was under a spring tide cycle (0.0003 m/s).

The longitudinal Stokes drift, V_2, was an order of magnitude lower than the Eulerian current, V_1, in most of the tidal cycles, with a mean value of 0.004 m/s for Agiasma, 0.003 m/s for Porto Lagos, and 0.003 m/s for Xirolimni. The Stokes drift effect was always positive at the Agiasma channel; hence, the water flowed into the lagoon. There was an exception in Xirolimni during the 27 April 2018 spring tidal cycle, when the Stokes drift effect prevailed over the Eulerian current.

Table 8. Residual fluxes and total transport rates (per unit of width) of nitrogen, total phosphorus and chlorophyll-a during the sampled tidal cycles at the mouth of the three lagoons under study.

Date	Tidal Phase	Nitrogen Residual Fluxes			Total Phosphorus Residual Fluxes			Chlorophyll-a Residual Fluxes		
		$V_{N,1}$	$V_{N,2}$	$<Q_N>$	$V_{TP,1}$	$V_{TP,2}$	$<Q_{TP}>$	$V_{Chl\text{-}a,1}$	$V_{Chla\text{-}a,2}$	$<Q_{Chla\text{-}a}>$
Agiasma										
29 September 2016	S	−6.42	0.02	−10.09	−4.45	0.09	−6.87	−0.14	0.01	−0.21
30 September 2016	S	−5.93	−0.72	−10.64	−3.13	0.08	−4.88	−0.21	0.02	−0.30
mean		−6.18	−0.35	−10.37	−3.79	0.09	−5.88	−0.18	0.02	−0.26
Porto Lagos										
26 June 2018	S	−4.41	5.41	2.04	−1.00	0.19	−1.66	−0.06	−0.04	−0.19
06 July 2018	N	1.53	1.34	14.41	0.70	0.66	6.82	0.12	0.32	2.19
10 July 2018	N	0.94	0.27	4.19	1.11	0.93	7.05	0.26	−0.09	0.61
mean		−0.65	2.34	6.88	0.27	0.59	4.07	0.11	0.06	0.87
Xirolimni										
19 July 2016	S	−5.26	−0.69	−11.18	−3.60	−2.04	−10.61	−0.04	−0.01	−0.10
26 July 2016	N	−2.56	−3.38	−11.41	−0.50	−0.99	−2.87	−0.03	0.07	0.07
30 April 2018	S	−7.87	1.43	−15.33	−1.70	−0.38	−4.94	−0.01	0.01	0.001
01 May 2018	S	4.88	5.00	23.77	1.39	0.74	5.12	0.01	0.01	0.04
01 May 2018	S	−1.62	2.64	2.38	−0.87	−3.71	−10.70	0.001	−0.01	−0.02
mean		−2.49	1.00	−2.35	−1.06	−1.28	−4.80	−0.01	0.01	−0.002

Positive values represent fluxes towards the lagoon and negative values away from the lagoon. $V_{N,1}$ and $V_{N,2}$, $V_{TP,1}$ $V_{TP,2}$, $V_{Chl\text{-}a,1}$, and $V_{Chla\text{-}a,2}$ in mg/(m^{2}s); $<Q_N>$, $<Q_{TP}>$, and $<Q_{Chla\text{-}a}>$ in (mg/(ms)).

The advection of mean salinity by the flow of water was the main mechanism of salt flux through the inlets of the three lagoons. The residual flux of salt due to the water flow, $V_{s,1}$, had an absolute mean value of 2.199 g/(m^{2}s) for Agiasma, 0.408 g/m^{2}s) for Porto Lagos, and 1.346 g/(m^{2}s) for Xirolimni. In Agiasma, $V_{s,1}$ had negative values during all the sampled cycles, indicating that the salt was transported from the lagoon out to the sea. In Porto Lagos, $V_{s,1}$ obtained the higher value during the spring tidal cycle (0.678 g/(m^{2}s)), showing direction out of the lagoon, while the two neap cycles showed lower values with direction into the lagoon. In Xirolimni, $V_{s,1}$ had the higher value during the 19 July 2016 spring tidal cycle (1.921 g/(m^{2}s)) and the lowest value during the 01 May 2018 spring tidal cycle (0.705 g/(m^{2}s)). $V_{s,1}$ pushed water out of the lagoon in most cycles in Xirolimni lagoon except for three of them, where the salt flux $V_{s,1}$ moves into the lagoon.

The salt flux due to tidal pumping mechanism was found to be highly important for the salt exchange of these lagoons, but it was found an order of magnitude lower than $V_{S,1}$ (mean values: $V_{s,2}$ = 0.199 g/(m^{2}s) for Agiasma, $V_{s,2}$ = 0.040 g/(m^{2}s) for Porto Lagos, and $V_{s,2}$=0.113 g/(m^{2}s) for Xirolimni). $V_{s,2}$ values were positive for the studied cycles for the three lagoons, which means that salt was pushed into the lagoons due to the Stokes drift effect.

DIN, total phosphorus, and chlorophyll-a appear to be pushed in and out of the lagoons due to both residual processes. The advection transport of nitrogen, total phosphorus, and chlorophyll-a have a mean value of –6.18 mg/(m^{2}s), –3.79 mg/(m^{2}s), and –0.18 mg/(m^{2}s), respectively, for Agiasma; –0.65 mg/(m^{2}s), 0.27 mg/(m^{2}s), and 0.11 mg/(m^{2}s), respectively, for Porto Lagos; and –2.49 mg/(m^{2}s), –1.06 mg/(m^{2}s), and –0.01 mg/(m^{2}s), respectively, for Xirolimni. It is mostly negative for the three lagoons throughout the sampled cycles. Advection transport and Stokes drift seem to be of the same order of magnitude for Porto Lagos and Xirolimni, whereas the Stokes drift was assessed to be an order of magnitude lower for Agiasma.

3.3. Tidal Prisms and Residence time

Lagoons' tidal prisms were calculated following the Equations (10) and (11) during flood and ebb periods. Results for the three lagoons are shown in Table 9. The mean volume of flood and ebb water was 10,100 m^3 and 173,350 m^3 for Agiasma, 38,030 m^3 and 52,730 m^3 for Porto Lagos, and 60,690 m^3 and 113,810 m^3 for Xirolimni per meter channel width. The average tidal prism for Agiasma was 1,830,000 m^3 for Agiasma, 610,000 m^3 for Porto Lagos, and 1,400,000 m^3 for Xirolimni.

Table 9. Water volumes per unit of width during flood and ebb in the lagoons under study.

Date	Tidal Phase	V_{Flood} ($\times 10^3$ m^3/m)	V_{Ebb} ($\times 10^3$ m^3m)	V_{Prism} ($\times 10^6$ m^3)	V_R ($\times 10^6$ m^3)	Q_R (m^3/s)	Return Flow Factor b	Flushing Time (d)
Agiasma								
29 September 2016	S	20.38	197.60	2.13	0.28	5.92	0.071	0.98
30 September 2016	S	2.06	132.36	1.31	0.37	9.78	0.166	1.00
30 September 2016	S	7.85	202.08	2.05	0.61	12.38	0.175	1.03
mean		10.10	177.35	1.83	0.42	9.36	0.137	1.00
Porto Lagos								
26 June 2018	S	75.26	141.73	1.43	0.02	0.47	0.008	1.15
06 July 2018	N	21.03	10.77	0.21	0.02	0.43	0.046	3.71
10 July 2018	N	17.80	5.69	0.19	0.01	0.24	0.024	4.23
mean		38.03	52.73	0.61	0.02	0.38	0.026	3.03
Xirolimni								
19 July 2016	S	81.75	209.89	2.35	0.07	1.41	0.015	0.80
20 July 2016	S	8.80	333.06	2.75	0.07	1.56	0.012	0.65
20 July 2016	S	64.08	155.85	1.77	0.04	0.92	0.012	0.81
26 July 2016	N	110.95	108.57	1.77	0.04	0.80	0.011	0.80
27 July 2016	N	91.05	75.22	1.34	0.04	0.82	0.013	0.82
27 July 2016	N	106.42	34.87	1.14	0.02	0.52	0.010	0.91
27 April 2018	S	86.23	56.50	1.15	0.07	1.62	0.031	0.89
28 April 2018	S	91.12	33.91	1.01	0.06	1.37	0.033	1.02
28 April 2018	S	59.20	67.78	1.02	0.06	1.35	0.030	0.97
29 April 2018	S	27.86	77.02	0.84	0.05	1.09	0.031	1.12
29 April 2018	S	24.64	177.18	1.62	0.10	2.13	0.031	0.81
30 April 2018	S	10.83	94.90	0.85	0.05	1.25	0.030	0.96
30 April 2018	S	38.72	197.63	1.90	0.11	2.62	0.031	0.75
01 May 2018	S	29.79	9.52	0.32	0.02	0.45	0.031	1.87
01 May 2018	S	78.90	75.26	1.24	0.07	1.65	0.031	0.90
mean		60.69	113.81	1.40	0.06	1.30	0.023	0.94

Agiasma received the higher amount of freshwater, with a mean value of 420,000 m^3, followed by Xirolimni (60,000 m^3) and Porto Lagos (20,000 m^3). The highest freshwater influx was recorded in Agiasma on 30/09/2016 (610,000 m^3), which corresponds to a discharge of 12.38 m^3/s. Following Equation (17), the return flow factor was calculated. It ranged between 0.008 under limited freshwater input to 0.175 under increased freshwater discharge. Solving Equation (18), the lagoons' residence time was computed. A mean residence time of 1 day was estimated for Agiasma lagoon, 3.03 days for Porto Lagos, and 0.94 days for Xirolimni. In the Porto Lagos lagoon, the residence time ranged from 1.15 days during the 26/06/2018 spring tidal period to 4.23 days during the 06 July 2018 neap tidal period (Table 9). In Xirolimni lagoon, the residence time ranged from 0.80 to 0.91 days under neap tidal cycles and 0.75 to 1.87 days under spring conditions.

The relative contribution of barotropic, baroclinic, and wind-induced exchange mechanisms to the overall salt-transport processes through the mouth of the lagoons are presented in Table 10. The barotropic tidal exchange rate prevails in all three lagoons, while the baroclinic exchange rate is insignificant. The wind-induced exchange rate is stronger for the Porto Lagos lagoon and lower for Xirolimni.

Table 10. Relative contribution of barotropic, baroclinic, and wind-induced exchange mechanisms.

Lagoon	R_{Tide} (1/day)	$R_{Baroclinic}$ (1/day)	R_{Wind} (1/day)
Agiasma	2.09	~0	0.010
Porto Lagos	0.78	~0	0.040
Xirolimni	3.01	~0	0.009

4. Discussion

Agiasma, Porto Lagos, and Xirolimni are Mediterranean coastal systems connected with the adjacent open sea through their inlet canals. The water, salt, and nutrient exchange processes greatly affect the delicate ecological balance and the carrying capacity of these systems. Tidal variability and non-tidal factors affect the intra- and inter-tidal exchanges between the lagoon and the open sea [29]. These lagoons are microtidal with limited freshwater entering directly from precipitation and agricultural drainage. Vertical stratification is infrequent and extremely weak or non-existent, and the gravitational circulation prevails due to the pressure gradient between the open sea and the lagoon. Previous studies suggested that the weak longitudinal salinity gradient may produce low baroclinic forcing at the mouth of a lagoon [9], and our results are in accordance with this observation.

One of the goals of this study was to identify the relative importance of physical processes (tidal, hydrologic, and meteorological) responsible for the overall exchange of water masses between the lagoon and the adjacent sea. Our findings illustrate that tides are the prevailing mechanism for the longitudinal distribution of water, salt, and chemical parameters. The local forcing by wind shear stress was shown to be the secondary factor. Asymmetrical tidal velocities were observed during most tidal cycles for the three lagoons, with velocities during ebbs being higher in most of the cycles than those during floods. Such ebb-dominance favors the entry of fish inside the lagoon at the post-larval stage and supports fishery activities in these systems.

Present results are in agreement with the findings of Sylaios, et al. [9] in Vassova lagoon. Nador lagoon in Morocco is another ebb-dominated micro-tidal system, especially after its old inlet was closed, and a new, wider, and deeper entrance was opened [30]. In Agiasma and Porto Lagos, during the spring tidal cycles, ebb periods were longer, covering about 60% of the tidal cycle, while during neap cycles, the flood dominated. This pattern was not observed in Xirolimni, where the neap tide cycles and five of the spring cycles were ebb-dominated. Flood and ebb duration asymmetry is also monitored in the Vassova lagoon [18]. Those velocity asymmetries under a semi-diurnal tidal signal could occur due to the non-linear effects induced by bottom friction [31] and the occurrence of non-tidal effects [32]. Velocity asymmetry will also influence the suspended sediment transport in and out of the lagoon, affecting the long-term inlet morphodynamics [29]. In the studied lagoons, ebb-dominated flow at the inlet leads to the development of an ebb shoal at the shelf side of the inlet (Figure 6). This sediment shoal could also affect the tidal and residual circulation of these systems, as in Price Inlet, California [33].

The net longitudinal currents and fluxes of water and salt were analyzed, showing that the Eulerian residual currents pushed the water out of the lagoons in 71% of the cycles, with Agiasma having the higher Eulerian current values. As expected, the Stokes drift effect was found an order of magnitude smaller than the Eulerian current, as it is significant in estuarine inlets with larger ratios of tidal range to mean depth. Stokes drift transported the water into the Agiasma lagoon, but for the other two lagoons, both directions occurred. As explained by Smith [34], these physical processes are affected by inlet configuration and dimensions, lagoon size, and orientation with respect to prevailing winds and water depth. Residual processes are seasonally variable due to the changes in the dominant winds, freshwater influxes, and evaporative losses throughout the year.

Figure 6. Ebb shoal developed by the sediment transport at the shelf side of the inlet induced by the ebb-dominated currents (Agiasma lagoon).

The water volumes leaving the lagoon during ebb were found higher in most of the cycles. The same phenomena was observed at the Mondego estuary [35], Vassova lagoon [9], and Obidos lagoon [35], where the residual water volumes were found positive. Specifically, in the Agiasma lagoon, the ebb residual volumes were significantly higher compared to the flood residual volumes. In Porto Lagos, during the neap tides, the flood residual volumes exceeded the ebb ones. In Xirolimni, ebb residual volumes exceed the flood ones under neap tides and during some of the spring tides. In such ebb-dominated inlets, the lagoon mouth is more effective in its water exchange at the low than at the high tide.

Since these lagoons receive limited freshwater influx, especially during autumn and winter storms, inreased concentrations in nutrients and chlorophyll-a are found in the main basins. The exiting loads of nutrient and chlorophyll-a during the ebb phase were higher during spring tides but lower during neap tides. A spring tidal cycle in Xirolimni appears to be an exception, as the flood loads of the dissolved constituents were found higher than the ebb fluxes.

The return flow factor was found at rather low levels, with the Agiasma lagoon showing the highest values among the studied lagoons. Agiasma also received the largest amount of freshwater, equal to 9.36 m^3/s compared to Xirolimni (1.30 m^3/s) and Porto Lagos (0.38 m^3/s). The highest residence time was computed at Porto Lagos lagoon

(3.03 days). Soria, et al. [15] calculated the residence time of Albufera of Valencia, a coastal lagoon in Spain, which receives significant amounts of surface water, to be 28.7 to 49.9 days. They concluded that the surface water inflow decreased during the last 30 years, which led to the increase of residence time. On the other hand, in the Mondego estuary and Obidos lagoon, the residence time varied from 2 days in winter to 5 days in summer and 3 days in winter to 4 days in summer, respectively [35]. The residence time is lower during winter due to higher river discharge.

Residence time, normalized by the prevailing tidal period, was found to be correlated to the tidal prism exchanged as the fraction of the lagoon volume, with the following power function fitted on the data (R^2 = 0.99) (Figure 7):

$$\ln\left(\frac{t_{RES}}{T}\right) = 0.70 - 0.50\ln\left(\frac{V_{Prism}}{V_{Lagoon}}\right) + 0.11\left(\ln\left(\frac{V_{Prism}}{V_{Lagoon}}\right)\right)^2 \quad (24)$$

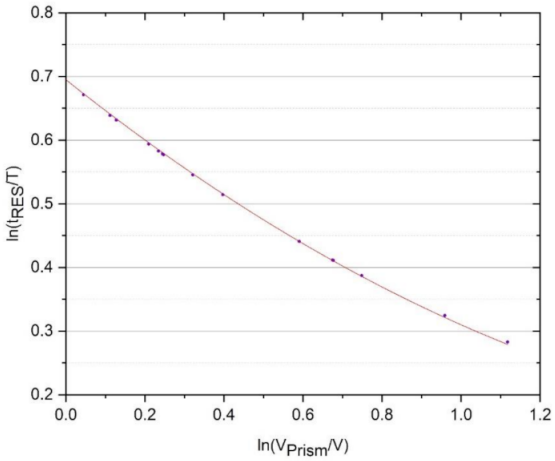

Figure 7. Normalized relations between lagoons' residence time (t_{RES}/T) to lagoon water exchange (V_{Prism}/V_{Lagoon}).

Similarly, in Figure 8, our summarized findings on lagoons' normalized residence time indicate a non-linear correlation with the barotropic tidal exchange (R^2 = 0.99) by:

$$\ln(\frac{t_{RES}}{T}) = 1.09 - 0.68\ln(R_{Tide}) + 0.13(\ln(R_{Tide}))^2 \quad (25)$$

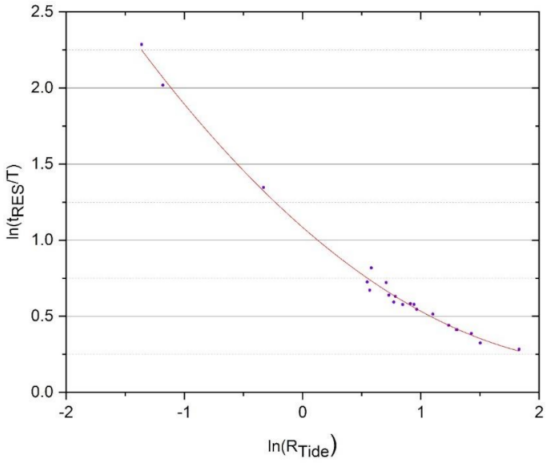

Figure 8. Normalized relations between lagoons' residence time (t_{RES}/T) to barotropic exchange component (R_{Tide}).

5. Conclusions

Agiasma, Porto Lagos, and Xirolimni are small-sized microtidal systems with limited freshwater influx from precipitation and agricultural runoff. The goal of this study was to determine the mechanisms responsible for the intra-tidal and residual movements of water, salt, nutrients, and chlorophyll at the inlet of three lagoons and their residence time.

Tides appear to be the controlling factor for the longitudinal exchange of the physical and chemical parameters, followed by wind stress. The baroclinic exchange rate is almost negligible due to the limited amount of freshwater received.

The Eulerian residual currents push water outwards in most of the sampled cycles, while the Stokes drift effect transports water into the Agiasma lagoon, but for the other two lagoons, both directions occurred. The Stokes drift was calculated an order of magnitude smaller than the Eulerian mechanism. The nitrogen, total phosphorus, and chlorophyll-a Stokes drift were also found reaching an order of magnitude lower than the Eulerian residual transport for Agiasma lagoon, while in Porto Lagos and Xirolimni, they appeared of similar magnitude.

The mean tidal prism during ebb was found higher than the corresponding mean flood tidal prism. This means that as these lagoons receive nutrients from agricultural drainages, part of these nutrients are exported to the coastal waters during ebb. The mean residence time was found ~1 day for Agiasma and Xirolimni and 3 days for Porto Lagos. This work produced non-dimensional relations between the residence time of these lagoons and their exchange characteristics as expressed by the tidal prism and the barotropic effect.

In the current study on the water, salt, and nutrient exchange, the estimation of fluxes and the assessment of lagoons' residence time should be related to the current ecological state of the lagoons and could be used as a tool for their management and restoration. Restoration actions should target adjusting the geometry of the inlet canals, such as an increase of its width or its depth, or opening of a second one. Those actions will be able to promote water exchange with the adjacent sea and improve lagoon water quality.

Author Contributions: Conceptualization, M.Z. and G.S.; methodology, G.S.; software, N.K.; validation, G.S.; formal analysis, M.Z.; resources, G.S.; data curation, M.Z. and N.K.; writing—original draft preparation, M.Z.; writing—review and editing, G.S.; visualization, N.K.; supervision, G.S. All authors have read and agreed to the published version of the manuscript.

Funding: This research received no external funding.

Institutional Review Board Statement: This study did not require an approval by DUTH Ethics Committee.

Informed Consent Statement: Not Applicable.

Data Availability Statement: Not Applicable.

Conflicts of Interest: The authors declare no conflict of interest.

Abbreviations

List of Symbols

Symbols	Explanation	Units
Q	instantaneous rate of water transport per unit of width through a water column	$m^3/(ms)$
H	mean depth of the lagoon	m
U	longitudinal velocity	m/s
u	longitudinal velocity in the x direction	m/s
v	longitudinal velocity in the y direction	m/s
$\langle Q \rangle$	tidally averaged residual rate of water transport	m^2/s

$\langle H \rangle$	tidally averaged depth of the lagoon	m
V_1	depth-averaged Eulerian residual transport	m/s
V_2	the mass transport Stokes drift transport	m/s
Q_S	instantaneous transport rate of salt	g/(ms)
S	water salinity	psu
$V_{s,1}$	depth-averaged residual flux of salt due to the residual transport of water	g/(m^{2}s)
$V_{s,2}$	depth-averaged residual flux due to tidal pumping	g/(m^{2}s)
$V_{s,3}$	depth-averaged residual flux of salt due to the vertical shear between the tidal and residual currents	g/(m^{2}s)
U'	deviations of velocity from the depth averaged value	m/s
S'	deviations of salinity from the depth averaged value	psu
$FloodVolume$	tidal prism during flood period per meter of width	m^3/m
$EbbVolume$	tidal prism during ebb period per meter of width	m^3/m
$PrismVolume$	lagoon tidal prism	m^3/m
T	tidal period	s
V_{Prism}	lagoon tidal prism volume	m^3
V_{Lagoon}	volume of the lagoon	m^3
S_{HW}	salinity in the lagoon at high tide	psu
S_{OC}	salinity of the open sea adjacent to the lagoon	psu
V_R	freshwater volume entering the lagoon during a tidal cycle	m^3
f	average fraction of fresh water by volume	
Q_R	fresh water inflow to the tidal flow	m^3/m
θ	flood and ebb flow lags because of the presence of river flow	
b	return flow factor	
R_{Tide}	barotropic tidal exchange rate	1/s
μ	retention coefficient	
$V_{Channel}$,	volume of the entrance canal	m^3
t_{Tide}	dominant tidal period	s
$R_{Baroclinic}$	baroclinic tidal exchange	1/s
A_c	cross-section area of the channel	m^2
$\Delta\rho$	density difference between the two ends of the entrance canal	kg/m^3
ρ	mean water density	kg/m^3
$h_{Channel}$	average depth of the channel and	m
g	acceleration due to gravity	m/s^2
R_{wind}	wind-induced exchange	1/s
t_{Wind}	period of wind forcing	s
V_{wind}	volume exchange produced by wind	m^3
$\Delta\eta$	elevation difference between the two ends of the entrance canal	m
β	fraction of wind stress that is balanced by pressure gradient	
C_W	wind drag coefficient	
ρ_{air}	air density	kg/m^3
L,	length of the lagoon basin	m
U	longitudinal component of wind vector	m/s
W	wind speed	m/s

References

1. Newton, A.; Brito, A.C.; Icely, J.D.; Derolez, V.; Clara, I.; Angus, S.; Schernewski, G.; Inácio, M.; Lillebø, A.I.; Sousa, A.I.; et al. Assessing, quantifying and valuing the ecosystem services of coastal lagoons. *J. Nat. Conserv.* **2018**, *44*, 50–65. [CrossRef]
2. Pérez-Ruzafa, A.; Morkune, R.; Marcos, C.; Pérez-Ruzafa, I.M.; Razinkovas-Baziukas, A. Can an oligotrophic coastal lagoon support high biological productivity? Sources and pathways of primary production. *Mar. Environ. Res.* **2020**, *153*, 104824. [CrossRef]
3. Busch, M.; La Notte, A.; Laporte, V.; Erhard, M. Potentials of quantitative and qualitative approaches to assessing ecosystem services. *Ecol. Indic.* **2012**, *21*, 89–103. [CrossRef]
4. Enjolras, G.; Boisson, J.-M. Valuing lagoons using a meta-analytical approach: Methodological and practical issues. *J. Environ. Plan. Manag.* **2010**, *53*, 1031–1049. [CrossRef]

5. Imaz-Lamadrid, M.A.; Wurl, J.; Ramos-Velázquez, E. Future of Coastal Lagoons in Arid Zones under Climate Change and Anthropogenic Pressure. A Case Study from San Jose Lagoon, Mexico. *Resources* **2019**, *8*, 57. [CrossRef]
6. Koutrakis, E.; Sylaios, G.; Kamidis, N.; Markou, D.; Sapounidis, A. Fish fauna recovery in a newly re-flooded Mediterranean coastal lagoon. *Estuar. Coast. Shelf Sci.* **2009**, *83*, 505–515. [CrossRef]
7. Gačić, M.; Kovačević, V.; Mazzoldi, A.; Paduan, J.; Arena, F.; Mosquera, I.M.; Gelsi, G.; Arcari, G. Measuring water exchange between the Venetian Lagoon and the open sea. *Eos Trans. Am. Geophys. Union* **2002**, *83*, 217–222. [CrossRef]
8. de Brito, A.N., Jr.; Fragoso, C.R., Jr.; Larson, M. Tidal exchange in a choked coastal lagoon: A study of Mundaú Lagoon in northeastern Brazil. *Reg. Stud. Mar. Sci.* **2018**, *17*, 133–142. [CrossRef]
9. Sylaios, G.K.; Tsihrintzis, V.A.; Akratos, C.; Haralambidou, K. Quantification of Water, Salt and Nutrient Exchange Processes at the Mouth of A mediterranean Coastal Lagoon. *Environ. Monit. Assess.* **2006**, *119*, 275–301. [CrossRef] [PubMed]
10. Kjerfve, B.; Magill, K.E. Geographic and hydrodynamic characteristics of shallow coastal lagoons. *Mar. Geol.* **1989**, *88*, 187–199. [CrossRef]
11. Tamborski, J.; van Beek, P.; Rodellas, V.; Monnin, C.; Bergsma, E.; Stieglitz, T.; Heilbrun, C.; Cochran, J.K.; Charbonnier, C.; Anschutz, P.; et al. Temporal variability of lagoon–sea water exchange and seawater circulation through a Mediterranean barrier beach. *Limnol. Oceanogr.* **2019**, *64*, 2059–2080. [CrossRef]
12. Ferrarin, C.; Umgiesser, G.; Roland, A.; Bajo, M.; De Pascalis, F.; Ghezzo, M.; Scroccaro, I. Sediment dynamics and budget in a microtidal lagoon—A numerical investigation. *Mar. Geol.* **2016**, *381*, 163–174. [CrossRef]
13. Takeoka, H. Exchange and transport time scales in the Seto Inland Sea. *Cont. Shelf Res.* **1984**, *3*, 327–341. [CrossRef]
14. Cucco, A.; Umgiesser, G. Modeling the Venice Lagoon residence time. *Ecol. Model.* **2006**, *193*, 34–51. [CrossRef]
15. Soria, J.; Vera-Herrera, L.; Calvo, S.; Romo, S.; Vicente, E.; Sahuquillo, M.; Sòria-Perpinyà, X. Residence Time Analysis in the Albufera of Valencia, a Mediterranean Coastal Lagoon, Spain. *Hydrology* **2021**, *8*, 37. [CrossRef]
16. Sanford Lawrence, P.; Boicourt William, C.; Rives Stephen, R. Model for Estimating Tidal Flushing of Small Embayments. *J. Waterw. Port Coast. Ocean. Eng.* **1992**, *118*, 635–654. [CrossRef]
17. Luketina, D. Simple Tidal Prism Models Revisited. *Estuar. Coast. Shelf Sci.* **1998**, *46*, 77–84. [CrossRef]
18. Sylaios, G.K.; Tsihrintzis, V.A.; Akratos, C.; Haralambidou, K. Monitoring and Analysis of Water, Salt and Nutrient Fluxes at the Mouth of a Lagoon. *Water Air Soil Pollut. Focus* **2004**, *4*, 111–125. [CrossRef]
19. Sylaios, G.; Theocharis, V. Hydrology and Nutrient Enrichment at Two Coastal Lagoon Systems in Northern Greece. *Water Resour. Manag.* **2002**, *16*, 171–196. [CrossRef]
20. Tsihrintzis, V.A.; Sylaios, G.K.; Sidiropoulou, M.; Koutrakis, E.T. Hydrodynamic modeling and management alternatives in a Mediterranean, fishery exploited, coastal lagoon. *Aquac. Eng.* **2007**, *36*, 310–324. [CrossRef]
21. Zoidou, M.; Sylaios, G. Ecological risk assessment of heavy metals in the sediments of a Mediterranean lagoon complex. *J. Environ. Health Sci. Eng.* **2021**, *19*, 1835–1849. [CrossRef] [PubMed]
22. Apha Awwa, W. *Standard methods for the examination of water and wastewater*, 20th ed.; American Public Health Association; American Water Work Association; Water Environment Federation: Washington, DC, USA, 1998.
23. Uncles, R.J.; Jordan, M.B. Residual fluxes of water and salt at two stations in the Severn Estuary. *Estuar. Coast. Mar. Sci.* **1979**, *9*, 287–302. [CrossRef]
24. Dyer, K.R.; Lasta King, H. The Residual Water Flow through the Solent, South England. *Geophys. J. Int.* **1975**, *42*, 97–106. [CrossRef]
25. Hunter, J.R. *An investigation into the circulation of the Irish Sea*; 72-1; University College of North Wales, Marine Science Laboratories: Menai Bridge, UK, 1972; p. 166.
26. Tee, K.T. Tide-Induced Residual Current—Verification of a Numerical Model. *J. Phys. Oceanogr.* **1977**, *7*, 396–402. [CrossRef]
27. Uncles, R.J.; Elliott, R.C.A.; Weston, S.A.; Pilgrim, D.A.; Ackroyd, D.R.; McMillan, D.J.; Lynn, N.M. Synoptic Observations of Salinity, Suspended Sediment and Vertical Current Structure in a Partly Mixed Estuary. In *Physics of Shallow Estuaries and Bays*; van de Kreeke, J., Ed.; American Geophysical Union: Washington, DC, USA, 1986; pp. 58–70. [CrossRef]
28. Hearn, C.J.; Robson, B.J. On the effects of wind and tides on the hydrodynamics of a shallow mediterranean estuary. *Cont. Shelf Res.* **2002**, *22*, 2655–2672. [CrossRef]
29. Hoque, M.A.; Ahad, B.G.; Saleh, E. Hydrodynamics and suspended sediment transport at tidal inlets of Salut Mengkabong Lagoon, Sabah, Malaysia. *Int. J. Sediment Res.* **2010**, *25*, 399–410. [CrossRef]
30. Maicu, F.; Abdellaoui, B.; Bajo, M.; Chair, A.; Hilmi, K.; Umgiesser, G. Modelling the water dynamics of a tidal lagoon: The impact of human intervention in the Nador Lagoon (Morocco). *Cont. Shelf Res.* **2021**, *228*, 104535. [CrossRef]
31. Aubrey, D.G.; Speer, P.E. A study of non-linear tidal propagation in shallow inlet/estuarine systems Part I: Observations. *Estuar. Coast. Shelf Sci.* **1985**, *21*, 185–205. [CrossRef]
32. Ranasinghe, R.; Pattiaratchi, C. Tidal inlet velocity asymmetry in diurnal regimes. *Cont. Shelf Res.* **2000**, *20*, 2347–2366. [CrossRef]
33. Fitzgerald, D.M.; Nummedal, D. Response characteristics of an ebb-dominated tidal inlet channel. *J. Sediment. Res.* **1983**, *53*, 833–845. [CrossRef]
34. Smith, N.P. Chapter 4 Water, Salt and Heat Balance of Coastal Lagoons. In *Elsevier Oceanography Series*; Kjerfve, B., Ed.; Elsevier: Amsterdam, The Netherlands, 1994.
35. Mendes, J.; Ruela, R.; Picado, A.; Pinheiro, J.P.; Ribeiro, A.S.; Pereira, H.; Dias, J.M. Modeling Dynamic Processes of Mondego Estuary and Óbidos Lagoon Using Delft3D. *J. Mar. Sci. Eng.* **2021**, *9*, 91. [CrossRef]